

Figure 2. Ellipticity change of BSA (222 nm) and pantolactone (219 nm) as a function of irradiation time of the xenon lamp, dependence of CD spectra of BSA on the irradiation time (inserted figure), and the temperature (Temp) change with the irradiation time (below): (O) native BSA, (□) BSA in 6 M guanidine, and (Δ) pantolactone. These three were measured by circulating water at 25 °C into the cell: (●) BSA in the cell which was kept at 65 °C. In the inserted figure, numerical values indicate irradiation time (min) of the xenon lamp (see text), and the dotted curve shows the CD spectrum of BSA denatured thermally at 65 °C. All data in this figure were measured with the cell with a light path length of 2 mm. Concentrations of BSA and pantolactone were 5.5×10^{-6} M and 0.032%, respectively.

a reflex mirror (M0) is set in a J-500 apparatus). Then, the cell was moved to another CD apparatus at appropriate intervals to measure the CD spectrum. Figure 2 shows the ellipticity change of BSA at 222 nm as a function of irradiation time of the xenon lamp and the dependence of its CD spectra on the irradiation time (inserted figure). In spite of circulating thermostatted water (25 °C) into the cell, the irradiation caused to ascend temperature of the sample part from 25 to 27 °C in the initial 1-min interval. However, it was unchanged thereafter (Figure 2). With an increase in the irradiation time, the ellipticity of BSA abruptly decreased at both 25 and 65 °C, although the ellipticity of pantolactone at 219 nm was almost unchanged. The change was not observed for BSA in 6 M guanidine. The ellipticity of the protein decreased at the same rate in sodium dodecyl sulfate (SDS), while it decreased more slowly in urea (not shown). The ellipticity change of BSA was smaller in urea than in SDS (not shown). The transformation of the CD spectrum induced by the present irradiation was apparently larger than that induced thermally at 65 °C (Figure 2). The CD spectra of BSA¹ and ribonuclease A² in various conditions can be well simulated by the curve-fitting method³ with reference CD spectra determined by Chen et al.⁴ The same reference spectra also gave a synthesized spectrum which excellently agreed with each experimental spectrum in Figure 2. The relative proportion of the α -helical structure was 18% for BSA irradiated for 45 min, as opposed to 66% in the native state.¹

The present results indicate that the protein structure is altered by the irradiation of light used in the CD apparatus. The effect is less significant in the usual CD measurements, which require only several minutes for one sample, than those demonstrated in Figures 1 and 2. However, when the sample is left for a while in the light path, this effect becomes significant. This is the occasion when an experimental condition is changed as the cell is left in the light path. Indeed, many investigators are apt to leave the CD cell in the light path, when they measure CD changes with time or when they change temperature in the thermal denaturation studies. If the samples such as BSA and myoglobin are left for 10 h in the light path, 10–20% of total ellipticity would decrease

(1) (a) Takeda, K.; Shigeta, M.; Aoki, K. *J. Colloid Interface Sci.* **1987**, *117*, 120. (b) Takeda, K.; Sasa, K.; Kawamoto, K.; Wada, A.; Aoki, K. *J. Colloid Interface Sci.* **1988**, *124*, 284.

(2) Takeda, K.; Sasa, K.; Nagao, M.; Batra, P. P. *Biochim. Biophys. Acta* **1988**, *957*, 340.

(3) (a) Greenfield, N.; Fasman, G. D. *Biochemistry* **1969**, *8*, 4108. (b) Yang, J. T.; Wu, C.-S. C.; Martinez, H. M. In *Methods in Enzymology*; Academic Press Inc.: Orlando, FL, 1986; Vol. 130, p 208.

(4) Chen, Y.-H.; Yang, J. T.; Chau, K. H. *Biochemistry* **1974**, *13*, 3350.

due to this effect. The present phenomenon should be necessarily taken into consideration in the CD studies of proteins.

Acknowledgment. The authors deeply thank Norimasa Takeuchi, Masanori Shibasaki, Hiroshi Hayakawa, Daisuke Nakamura, and Tatsushi Kasai of Jasco (Tokyo) and Humiaki Shibata of Jasco (Osaka) for their kind cooperation and helpful discussions.

Location of β -Sheet-Forming Sequences in Amyloid Proteins by FTIR

Kurt J. Halverson, Irving Sucholeiki, Ted T. Ashburn, and Peter T. Lansbury, Jr.*

Department of Chemistry
Massachusetts Institute of Technology
Cambridge, Massachusetts 02139

Received January 8, 1991

The deposition of proteinaceous amyloid is characteristic of Alzheimer's disease (AD)¹ and type II diabetes.² Analysis of these amyloid deposits, or plaques, by X-ray diffraction^{2,3} indicates that they are composed of fibrils which contain a structural motif that was first observed in the Bombyx mori silk fibril.⁴ A low-resolution model for this structure, known as the cross- β fibril, was proposed by Pauling^{4,5} but has not been significantly refined,⁵ due to the fact that amyloid-forming proteins are extremely insoluble and do not readily crystallize.⁶ Consequently, the intrastrand and interstrand interactions which direct formation of the constituent antiparallel β -sheet are not understood.^{7,8} Krimm has suggested that isotope labeling of specific amides could be useful for the location of secondary structure within a protein sequence by Fourier transform infrared spectroscopy (FTIR).⁹ Walters et al. have recently demonstrated that this approach is feasible for a complex, multiconformational peptide in solution.¹⁰ We have extended this approach to allow the observation of specific transition dipole coupling interactions which are characteristic of β -sheet structure in the solid state. These studies reveal the existence of irregularities in cross- β fibril structure which cannot be otherwise observed and are incompatible with the Pauling model.

Antiparallel β -sheet structure is easily distinguished by FTIR due to a splitting of the amide I absorption which is caused by strong interstrand and, to a lesser extent, intrastrand transition dipole coupling (TDC) interactions.^{9,11–13} This effect results in

(1) Halverson, K.; Fraser, P. E.; Kirschner, D. A.; Lansbury, P. T. *Biochemistry* **1990**, *29*, 2639.

(2) Nishi, M.; Sanke, T.; Nagamatsu, S.; Bell, G. I.; Steiner, D. F. *J. Biol. Chem.* **1990**, *265*, 4173.

(3) Kirschner, D. A.; Abraham, C.; Selkoe, D. J. *Proc. Natl. Acad. Sci. U.S.A.* **1986**, *83*, 503.

(4) Marsh, R. E.; Corey, R. B.; Pauling, L. *Biochim. Biophys. Acta* **1955**, *16*, 1.

(5) Arnott, S.; Dover, S. S.; Elliot, A. *J. Mol. Biol.* **1967**, *30*, 201.

(6) Lotz, B.; Gonthier-Vassal, A.; Brack, A.; Magoshi, J. *J. Mol. Biol.* **1982**, *156*, 345.

(7) (a) Salemme, F. R. *Prog. Biophys. Mol. Biol.* **1983**, *42*, 95. (b) Chou, K.-C.; Pottle, M.; Nemethy, G.; Ueda, Y.; Scheraga, H. A. *J. Mol. Biol.* **1982**, *162*, 89.

(8) (a) von Heijne, G.; Bomberg, C. *J. Mol. Biol.* **1977**, *117*, 821. (b) Lifson, S.; Sander, C. *J. Mol. Biol.* **1980**, *139*, 627.

(9) Krimm, S.; Bandekar, J. *Adv. Prot. Chem.* **1985**, *38*, 181.

(10) Tadesse, L.; Nazarbachi, R.; Walters, L. *J. Am. Chem. Soc.*, in press. We thank the authors for sharing their results with us prior to publication.

(11) Moore, W. H.; Krimm, S. *Biopolymers* **1976**, *15*, 2465.

(12) Moore, W. H.; Krimm, S. *Biopolymers* **1976**, *15*, 2439. The authors note that a 5-Å radius sphere accounts for a majority of the TDC interactions.

(13) The strength of TDC (ΔV) between two interacting dipoles can be estimated according to the following equation (α , β , and γ are angles which relate to the relative orientation of the dipoles, r = distance between the dipole centers).^{10,11}

$$\Delta V \propto \frac{\cos \alpha - 3 \cos \beta \cos \gamma}{r^3}$$

Table I. β -Sheet Amide I Peak Positions (cm^{-1}) for Peptide Films^a

peptides and labeled analogues	¹² C amide I	¹³ C amide I
LMVGGVIA (β 34-42) ^{1,c}	1628	
L34 ^c	1629	$\geq 1610^b$
V36	1637	1607
G37	1633	1610
G38 ^c	1631	1605
V39 ^c	1643	1610
V40	1648/1633	1607
I41	1631	1606
LMVGPVVIA ^c	1638	
G37 ^c	1639	1604 ^d
V40 ^c	1648	1611

^aThe error in these measurements is $\pm 1 \text{ cm}^{-1}$ for the ¹²C band and $\pm 2 \text{ cm}^{-1}$ for the ¹³C band. ^bThe ¹³C band is not resolved, therefore this is an estimated lower limit. ^cSee spectrum in Figure 1. ^dPeak position was determined by second derivative; $\pm 3 \text{ cm}^{-1}$.

absorption bands which appear at ca. 1695 cm^{-1} (w) and ca. 1625 cm^{-1} (s) (random coil and helical conformations, in which TDC is negligible, give a localized amide I absorption bands at $1660\text{--}1650 \text{ cm}^{-1}$).⁹ Isotopic replacement makes it possible to selectively observe a single amide I absorption and to assign it to a specific amide carbonyl. For a localized amide I mode, replacement of a ¹²C amide with a ¹³C amide will result in a decrease in the amide I absorption frequency by $35\text{--}40 \text{ cm}^{-1}$.¹⁴ This isotope-induced shift has been exploited for the purpose of spectral assignment¹⁵ and to enable the observation of short-lived local structures in a soluble polypeptide.¹⁰ For the strongly coupled amide I mode in an antiparallel β -sheet, the situation is more complex.^{11,12} Since the strength of TDC is very sensitive to the difference in vibrational frequency between the interacting dipoles, labeling with ¹³C at a specific site should effectively localize that amide I mode by greatly reducing its TDC to the neighboring ¹²C amides. At the same time, the overall coupling of the "residual" ¹²C amides will be reduced, resulting in a shift of the ¹²C amide I absorption band to higher frequency. This communication reports the first experimental demonstration of this effect, and its exploitation for the determination of β -sheet regions in amyloid proteins.

The nine amino acid peptide β 34-42 ($\text{H}_2\text{N}\text{-Leu}\text{-Met}\text{-Val}\text{-Gly}\text{-Gly}\text{-Val}\text{-Val}\text{-Ile}\text{-Ala}\text{-CO}_2\text{H}$) which represents the carboxyl terminus of the amyloid-forming protein (β /A4) of AD resembles the native protein in its insolubility and cross- β fibrillar structure.¹ FTIR analysis indicates that the β 34-42 amyloid fibrils consist predominantly of antiparallel β -sheet structure (see spectrum at top of Figure 1).¹ Seven ¹³C carbonyl-labeled analogues of β 34-42, each containing a single ¹³C-labeled amide,¹⁶ were analyzed by FTIR. In solution (1 M LiBr/THF¹), the ¹³C-labeled peptides gave virtually identical spectra, with ca. 1/8th of the amide I intensity shifted to lower absorption frequency (1660 to 1625 cm^{-1}). The magnitude of the isotope-induced shift (35 cm^{-1}) was expected for a localized amide I mode.¹⁴ In contrast, the spectra of the peptide films, which were shown to contain cross- β fibrillar structure,¹⁷ were different from each other (see Figure 1, Table I). With the exception of peptide L34, the ¹³C amide I band was resolved and anomalously intense. The frequencies of the ¹³C amide I absorption bands varied between 1605 cm^{-1} (G38) and ca. 1615 cm^{-1} (L34), consistent with the expected reduction in TDC (if every amide carbonyl carbon were replaced with ¹³C, an amide I absorption at ca. 1591 cm^{-1} would be pre-

(14) The magnitude of the isotope-induced shift for a localized AB stretch can be calculated by the following equation

$$\nu_{\text{AB}} = \frac{1}{2\pi} \sqrt{\frac{k}{\mu}}$$

with ν_{AB} = absorption frequency for AB stretch, k = force constant for AB stretch, and $\mu = M_A M_B / (M_A + M_B)$ (M_A = mass of atom A). For a ¹²C=O to ¹³C=O change, a shift of 37 cm^{-1} is calculated. Since the amide I absorption is not purely a CO stretch,⁹ the actual shift may be slightly smaller.

(15) Deber, C. *Macromolecules* 1974, 7, 47.

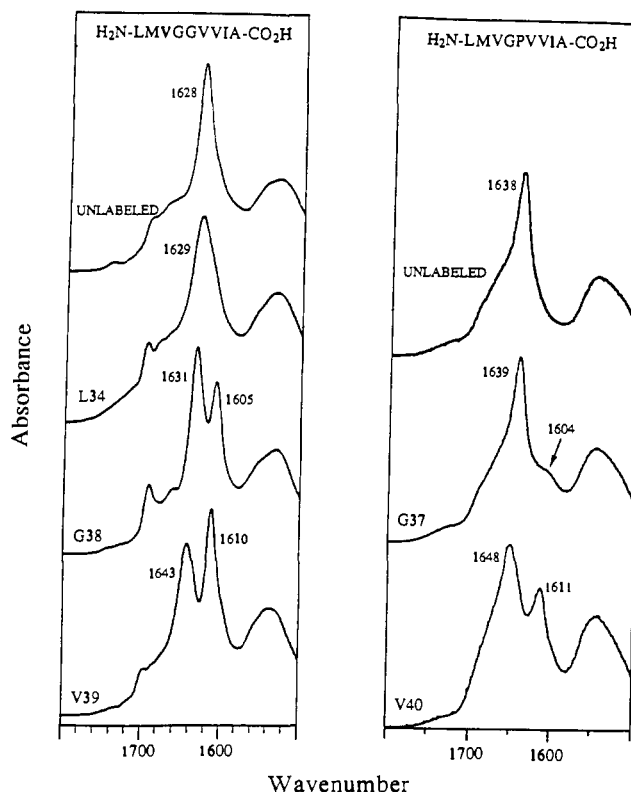


Figure 1. IR spectra of peptides LMVGGVIA (left panel) and LMVGPVVIA (right panel) in the film state.¹⁷ The spectra of the unlabeled peptides appear at the top of each panel. Labeled peptides are abbreviated according to the position of the ¹³C amide carbonyl carbon. The broad band at the low frequency end of the spectra as shown (ca. 1540 cm^{-1}) is the amide II band. Note the high frequency amide I band (ca. 1695 cm^{-1} for the unlabeled peptide) which is apparent in the spectra in the left panel. This band is diagnostic of antiparallel β -sheet.⁹

dicted).¹⁶ The differences in the ¹³C amide absorption frequencies reflect structural heterogeneity along the peptide backbone and intermolecular TDC between ¹³C amides. In order to remove the latter effect, each of the singly ¹³C-labeled β 34-42 analogues was diluted with unlabeled β 34-42 (1 part ¹³C peptide: 10 parts ¹²C peptide),¹⁷ resulting in film spectra in which the ¹³C band was shifted to higher frequency. This result indicates that the differences in the ¹³C amide I frequencies observed in the isotopically pure films are primarily due to intermolecular ¹³C-¹³C TDC.^{11,12} The location-dependent variation in the intermolecular TDC reflects the ordered nature of the aggregate.

Further examination of the film (β -sheet) spectra of the labeled analogues revealed that the residual ¹²C absorption band was shifted to higher frequency in each spectrum (see especially V39). This effect is due to the decrease in overall TDC brought about by the insertion of an off-resonance dipole and is diagnostic of β -sheet structure. The magnitude of the ¹²C frequency shift depends on the environment of the ¹³C amide, that is, strongly coupled (β -sheet) regions of the amyloid structure are more sensitive to isotopic replacement. We conclude that the valine

(16) Each labeled β 34-42 and LMVGPVVIA analogue peptide was synthesized and purified according to ref 1. Certain peptides (G37, V39, V40, I41) also contained ¹³C at an α carbon; however, this substitution was shown not to affect the spectrum in the amide I region. Each group of analogues was shown to coelute by reverse-phase HPLC,¹ and all peptides were characterized by FABMS. The position of the isotopic substitution(s) in each peptide was verified by MS-MS sequencing (we thank Dr. Ioannis Papanopoulos of the MIT Mass spectrometry facility, supported by NIH Division of Research Resources, Grant RR00317 to Prof. Klaus Biemann). IR spectra were measured on a Mattson Cygnus FTIR spectrophotometer. Second derivative analysis of the spectra was utilized in select cases.

(17) Thin films were formed by evaporating a formic acid solution of one peptide or, in the case of the dilution studies, a mixture of two weighed peptides onto a CaF₂ plate under a stream of argon or under vacuum. Films formed in this way have been shown by X-ray diffraction and/or electron microscopy to contain cross- β fibrillar structure.

residues (V36, V39, V40) are located in a β -sheet region of the aggregate, whereas the terminal residues, L34 and I41 (and A42) and the central residues, G37 and G38, are probably not part of an idealized β -sheet.

An analogue of β 34-42 in which Gly38 was replaced by Pro ($\text{H}_2\text{N-LMVGPPVIA-CO}_2\text{H}$) was synthesized with the intention of disrupting the amyloid-forming structure (ϕ 38 is restricted to $-60^\circ \pm 20^\circ$).¹⁶ This peptide formed fibrils¹⁷ but was more soluble than β 34-42. A film formed from LMVGPPVIA contained β -sheet (1638 cm^{-1}) and β -turn or random coil structure (ca. 1665 cm^{-1} , see Figure 1). Labeling at V40 led to a significant shift in the ^{12}C amide I band (1638 to 1648 cm^{-1}), whereas labeling of the G37 amide did not result in a similar shift (see Figure 1), suggesting that the V40 amide carbonyl is involved in the β -sheet structure and G37 is not.

These studies demonstrate that FTIR can be used to locate β -sheet (strongly coupled) structure in fibrillar proteins. Isotopic substitution within a β -sheet region reduces TDC, leading to a shift of the ^{12}C amide I absorption band to higher frequency. This shift is diagnostic for β -sheet structure; other structures do not produce this effect. The differences in the position of the ^{13}C amide I bands of the labeled β 34-42 analogues are due to deviations from idealized β -sheet structure and to intermolecular ^{13}C - ^{13}C dipole coupling. The latter effect could be exploited in order to elucidate the intermolecular interactions which drive aggregation.

Acknowledgment. We thank Dr. Lee Walters for stimulating our interest in FTIR and isotope labeling. We are grateful to Dr. Isao Noda, Dr. Tony Dowrey, Dr. Curt Marcott, Prof. Bob Field, Prof. Bob Silbey, Dr. Todd Miller, and Prof. Samuel Krimm for their insight and suggestions concerning this manuscript. This work was supported by Alzheimer's Disease Research (a program of the American Health Assistance Foundation, Rockville, MD), the Whitaker Health Sciences Fund, the National Institutes of Health (R01-AG08470-02), the National Science Foundation (Presidential Young Investigator Award), Merck & Co. (Faculty Development Grant), and the Camille and Henry Dreyfus Foundation (New Faculty Award).

Supplementary Material Available: The IR spectra discussed in this communication (6 pages). Ordering information is given on any current masthead page.

Electronic Tuning of Asymmetric Catalysts

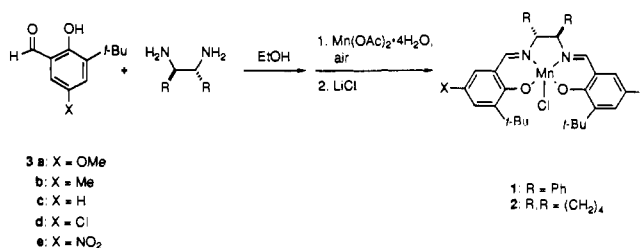
Eric N. Jacobsen,* Wei Zhang, and Mehmet L. Güler

Roger Adams Laboratory
Department of Chemistry
University of Illinois, Urbana, Illinois 61801

Received May 22, 1991

Although stereoelectronic control of π -facial diastereoselectivity has been recognized and evaluated in model systems,¹ this concept has not been successfully applied to the design of synthetically useful asymmetric catalysts. Indeed, the stereoselectivity of known

Scheme I



chiral reagents and catalysts is generally interpreted solely in terms of steric considerations. To our knowledge, the effect of varying the electronic properties of chiral catalysts has never been systematically assessed in practical systems,² although this is largely because known effective chiral catalysts tend not to be synthetically or structurally well-suited to electronic tuning. In contrast, chiral Mn^{III}salen epoxidation catalysts recently developed in our labs³ consist of a rigid and kinetically nonlabile ligand template wherein steric and electronic properties of the metal center may be tuned in a synthetically straightforward manner. We have taken advantage of this system to study substituent effects on alkene epoxidation, and we report examples of remarkable electronic control of enantioselectivity. This result may carry general implications for the design of new catalysts for reactions of unfunctionalized substrates.

Two series of catalysts were prepared from 1,2-diaminocyclohexane (catalysts **1a-e**) and from 1,2-diamino-1,2-diphenylethane (catalysts **2a-e**), respectively. Condensation of either of these diamines with the appropriate 5-substituted *tert*-butyl salicylaldehyde derivatives **3a-e** followed by insertion of the Mn(III) center as described previously^{3b} led to the requisite catalysts in excellent yield (Scheme I).⁴

We selected three model substrates for this study: 2,2-dimethylchromene (**4**), a member of a synthetically important class of olefins that is epoxidized with particularly high enantioselectivities with certain Mn^{III}salen catalysts;^{3c,5} *cis*- β -methylstyrene (**5**), an aryl-substituted alkene which has served as a model substrate for a variety of enzymatic and nonenzymatic epoxidation processes;⁶ and *cis*-2,2-dimethyl-3-hexene (**6**), an example of an aliphatically substituted alkene. As noted previously, *cis* disubstituted alkenes are generally the best substrates for chiral salen and porphyrin epoxidation catalysts.^{2a,3}

Each catalyst/substrate combination was examined under our previously described epoxidation conditions,⁷ and the results with catalyst **1** are presented in Hammett plots in Figure 1. In all cases the same trend was observed, with electron-donating groups on the catalyst leading to higher enantioselectivities in epoxidation. The effect is small with **6**, which is generally epoxidized with only marginal selectivity (26-37% enantiomeric excess), but it is particularly striking with **4**, where enantioselectivities (*ee*'s) range from 22% with **1e** to 96% for **1a**. This corresponds to a remarkable selectivity difference $\Delta\Delta G^\ddagger$ of 2.0 kcal/mol. Catalysts **2a-e**

(2) Electronic properties of substrate that have been shown in certain cases affect enantioselectivity with a given catalyst system. See, for example: (a) Groves, J. T.; Viski, P. *J. Org. Chem.* **1990**, *55*, 3628. (b) Naruta, Y.; Tani, F.; Maruyama, K. *Chem. Lett.* **1989**, 1269.

(3) (a) Zhang, W.; Loebach, J. L.; Wilson, S. R.; Jacobsen, E. N. *J. Am. Chem. Soc.* **1990**, *112*, 2801. (b) Zhang, W.; Jacobsen, E. N. *J. Org. Chem.* **1991**, *56*, 2296. (c) Jacobsen, E. N.; Zhang, W.; Muci, A. R.; Ecker, J. R.; Deng, L. *J. Am. Chem. Soc.* In press. See, also: Irie, R.; Noda, K.; Ito, Y.; Katsuki, T. *Tetrahedron Lett.* **1991**, *32*, 1055.

(4) All catalysts exhibited satisfactory analytical data (C, H, N, Cl, Mn).

(5) Lee, N. H.; Muci, A. R.; Jacobsen, E. N. *Tetrahedron Lett.* In press.

(6) (a) Ortiz de Montellano, P. R.; Fruetel, J. A.; Collins, J. R.; Camper, D. L.; Loew, G. H. *J. Am. Chem. Soc.* **1991**, *113*, 3195. (b) O'Malley, S.; Kodadek, T. *J. Am. Chem. Soc.* **1989**, *111*, 9116. See, also, refs 2a and 3b.

(7) Epoxidations were carried out at room temperature with aqueous commercial NaOCl buffered to pH 11.3 as the stoichiometric oxidant.^{3b} All *ee*'s were determined by capillary GC chromatography of crude reaction mixtures with a commercially available Cyclodex-B column (J & W Scientific, Folsom, CA 95630, 30 m \times 0.25 mm i.d., 0.25 μm film).

(1) (a) Cieplak, A. S.; Tait, B. D.; Johnson, C. R. *J. Am. Chem. Soc.* **1989**, *111*, 8447. (b) Halterman, R. L.; McEvoy, M. A. *J. Am. Chem. Soc.* **1990**, *112*, 6690. (c) Chung, W.-S.; Turro, N. J.; Srivastava, S.; Li, H.; le Noble, W. J. *J. Am. Chem. Soc.* **1988**, *110*, 7882.